

## Supporting Information for

*CrystEngComm*

### **Modulation of the Directions of the Anisotropic Axes of Dy<sup>III</sup> ions through Utilizing Two kinds of Organic Ligands or Replacing Dy<sup>III</sup> ions by Fe<sup>III</sup> ions**

Hui-Sheng Wang,<sup>\*a</sup> Yong Chen,<sup>a</sup> Zhao-Bo Hu,<sup>b</sup> Cheng-Ling Yin,<sup>a</sup> Zaichao Zhang<sup>\*c</sup> and Zhi-Quan Pan<sup>a</sup>

<sup>a</sup> School of Chemistry and Environmental Engineering, Key Laboratory of Green Chemical Process of Ministry of Education, Key Laboratory of Novel Reactor and Green Chemical Technology of Hubei Province, Wuhan Institute of Technology, Wuhan 430074, P. R. China.

<sup>b</sup> State Key Laboratory of Coordination Chemistry, School of Chemistry and Chemical Engineering, Collaborative Innovation Center of Advanced Microstructures, Nanjing University, Nanjing 210046, P. R. China.

<sup>c</sup> Jiangsu Key Laboratory for the Chemistry of Low-dimensional Materials, School of Chemistry and Chemical Engineering, Huaiyin Normal University, Huaian 223300, P. R. China.

Corresponding author, E-mail: wangch198201@163.com and zhangzc@hytc.edu.cn

## Contents

- Table S1.** Crystal data and structure refinement parameters for **1** and **2**.
- Table S2.** Selected bond lengths (Å) and angles (°) for **1**.
- Table S3.** Selected bond lengths (Å) and angles (°) for **2**.
- Table S4.** Bond valence sum (BVS) calculations for determining of the protonation levels of the O atoms in **1** and **2**.
- Table S5.** Bond valence sum (BVS) calculations for determining of the oxidation of the Fe atoms in **2**.
- Table S6.** The possible geometries of oct-coordination metal centers and Deviation parameters from each ideal polyhedron for Dy of complex **1**.
- Table S7.** The possible geometries of oct-coordination metal centers and Deviation parameters from each ideal polyhedron for Dy of complex **2**.
- Table S8.** Some [Fe<sub>4</sub>Dy<sub>2</sub>] complexes reported in recent years.
- Scheme S1.** The coordination modes of (py)<sub>2</sub>C(OH)O<sup>-</sup>, HL<sup>2-</sup> and NO<sub>3</sub><sup>-</sup> with metals for **1**.
- Scheme S2.** The coordination modes of L<sup>3-</sup>, HL<sup>2-</sup>, H<sub>2</sub>L<sup>-</sup> and H<sub>3</sub>L in the complexes with the formula [Fe<sup>III</sup><sub>4</sub>Ln<sup>III</sup><sub>2</sub>(H<sub>2</sub>L)<sub>2</sub>(HL)<sub>2</sub>L<sub>2</sub>(CH<sub>3</sub>OH)<sub>2</sub>((CH<sub>3</sub>)<sub>3</sub>CCOO)<sub>2</sub>(NO<sub>3</sub>)<sub>2</sub>] [Ln<sup>III</sup>(NO<sub>3</sub>)<sub>4</sub>(H<sub>3</sub>L)(CH<sub>3</sub>OH)]<sub>3</sub>·NO<sub>3</sub>·3H<sub>2</sub>O reported by J. Reedijk *et al.*
- Figure S1.** PXRD patterns and simulated patterns generated from single crystal diffraction data for compound **1**.
- Figure S2.** PXRD patterns and simulated patterns generated from single crystal diffraction data for compound **2**.
- Figure S3.** Plots of TGA for complexes **1** (left) and **2** (right). The red arrows were directed the weight losses or temperatures to see easily.
- Figure S4.** The plot shows the  $\pi$ - $\pi$  packing interactions and the shortest distances of Dy<sup>III</sup>...Dy<sup>III</sup> between the nearest neighboring molecules of **1**.
- Figure S5.** The plots show the  $\pi$ - $\pi$  stacked interactions (left) and the shortest distances of Fe<sup>III</sup>...Fe<sup>III</sup>, Fe<sup>III</sup>...Dy<sup>III</sup> and Dy<sup>III</sup>...Dy<sup>III</sup> between the nearest neighboring molecules of **2** (right).
- Figure S6.** The plots of the field dependence of the magnetization for **1** (left) and **2** (right) at different temperatures.
- Figure S7.** Plots of in-phase ( $\chi'$ ) versus  $T$  for **1** with a zero applied dc field. **Figure S8.** Plots of in-phase ( $\chi'_M$ ) versus  $T$  for **1** with a zero applied dc field.
- Figure S8.** Plots of in-phase ( $\chi'$ ) versus  $f$  (left) and out-of-phase ( $\chi''$ ) versus  $f$  (right) for **1** with a zero applied dc field.
- Figure S9.** Frequency dependence of the out-of-phase ( $\chi''$ ) ac magnetic susceptibilities for **2** collected under a 0 Oe dc field with the temperature 1.8.
- Figure S10.** Plots of out-of-phase ( $\chi''$ ) versus  $f$  for **1** (left) at 2.0 K and for **2** (right) at 1.8 K with the applied dc field shown in plots.
- Figure S11.** Plots of in-phase ( $\chi'$ ) versus  $T$  for **2** under a dc field of 1500 Oe.
- Figure S12.** Plots of in-phase ( $\chi'$ ) versus  $f$  (left) and out-of-phase ( $\chi''$ ) versus  $f$  (right) for **2** under a dc field of 1500 Oe.

**Table S1.** Crystal data and structure refinement parameters for **1** and **2**.

Compounds	<b>1</b>	<b>2</b>
-----------	----------	----------

Formula <sup>a</sup>	C <sub>74</sub> H <sub>82</sub> Dy <sub>4</sub> N <sub>15</sub> O <sub>20.50</sub>	C <sub>79</sub> H <sub>93</sub> Cl <sub>4</sub> Dy <sub>2</sub> Fe <sub>4</sub> N <sub>16</sub> O <sub>21.50</sub>
Formula weight <sup>a</sup>	2159.54	2300.89
Crystal colour	colorless	yellow
Crystal size/mm	0.23 × 0.18 × 0.11	0.43 × 0.08 × 0.04
Crystal system	monoclinic	monoclinic
Space group	<i>P</i> 2 <sub>1</sub> / <i>c</i>	<i>C</i> 2/ <i>c</i>
<i>a</i> (Å)	14.6108(6)	57.391(3)
<i>b</i> (Å)	17.6065(9)	13.9533(6)
<i>c</i> (Å)	31.2383(16)	24.8627(10)
$\alpha$ (°)	90.00	90
$\beta$ (°)	97.693(2)	115.2630(10)
$\gamma$ (°)	90.00	90
Unit cell volume (Å <sup>3</sup> )	7963.6(7)	18005.6(15)
Temperature (K)	173(2)	173(2)
<i>Z</i>	4	8
Wavelength (Å)	0.71073	0.71073
$\mu$ (Mo K $\alpha$ ) [mm <sup>-1</sup> ]	3.790	2.464
<i>D</i> <sub>c</sub> (g cm <sup>-3</sup> )	1.801	1.698
$\theta$ range (°)	3.0321-25.3256	2.9363-25.3964
Index ranges	-17 ≤ <i>h</i> ≤ 16 -18 ≤ <i>k</i> ≤ 20 -33 ≤ <i>l</i> ≤ 37	-68 ≤ <i>h</i> ≤ 68 -16 ≤ <i>k</i> ≤ 16 -29 ≤ <i>l</i> ≤ 27
<i>F</i> (000)	4236	9240
Reflections collected	43372	67001
Unique reflections [ <i>R</i> <sub>int</sub> ]	13903	15649
Reflections with <i>I</i> > 2 $\sigma$ ( <i>I</i> )	9219	10760
Final <i>R</i> indices ( <i>I</i> > 2 $\sigma$ ( <i>I</i> )) <sup>b,c</sup>	<i>R</i> <sub>1</sub> = 0.0655, <i>wR</i> <sub>2</sub> = 0.1026	<i>R</i> <sub>1</sub> = 0.0695, <i>wR</i> <sub>2</sub> = 0.1332
Final <i>R</i> indices (all data)	<i>R</i> <sub>1</sub> = 0.1191, <i>wR</i> <sub>2</sub> = 0.1135	<i>R</i> <sub>1</sub> = 0.1204, <i>wR</i> <sub>2</sub> = 0.1492
<i>S</i> (all data)	1.107	1.103
( $\Delta\rho$ ) <sub>max,min</sub> /e Å <sup>-3</sup>	1.847 and -1.502	2.341 and -2.190

<sup>a</sup> The formula and the formula weights include the H<sub>2</sub>O and MeCN solvent molecules which were subtracted by SQUEEZE program. <sup>b</sup>*R*<sub>1</sub> =  $\Sigma(|F_o| - |F_c|)/\Sigma|F_o|$ . <sup>c</sup> *wR*<sub>2</sub> =  $[\Sigma[w(F_o^2 - F_c^2)^2]/\Sigma[w(F_o^2)^2]]^{1/2}$ ,  $w = 1/[\sigma^2(F_o^2) + [(ap)^2 + bp]$ , where  $p = [\max(F_o^2, 0) + 2F_c^2]/3$ .

**Table S2.** Selected bond lengths (Å) and angles (°) for **1**.

Selected bond lengths for <b>1</b>					
Dy1-O1	2.197(8)	Dy2-O13	2.437(7)	Dy3-O13	2.568(7)
Dy1-O11	2.254(8)	Dy2-O17	2.488(7)	Dy3-O17	2.579(6)

Dy1-O2	2.304(7)	Dy2-N2	2.505(9)	Dy4-O10	2.258(7)
Dy1-O18	2.370(7)	Dy2-O15	2.505(7)	Dy4-O11	2.263(8)
Dy1-O15	2.460(7)	Dy2-N5	2.540(9)	Dy4-O8	2.264(7)
Dy1-N1	2.508(9)	Dy3-O7	2.211(7)	Dy4-O13	2.423(7)
Dy1-N7	2.534(9)	Dy3-O5	2.253(7)	Dy4-O15	2.443(7)
Dy1-O17	2.583(6)	Dy3-O8	2.302(7)	Dy4-N8	2.480(9)
Dy2-O4	2.252(7)	Dy3-O19	2.337(8)	Dy4-N4	2.507(10)
Dy2-O5	2.260(7)	Dy3-N3	2.507(9)	Dy4-O17	2.584(7)
Dy2-O2	2.276(7)	Dy3-N6	2.509(9)		

Selected bond angles for <b>1</b>					
O1-Dy1-O11	82.6(3)	O4-Dy2-O17	145.4(3)	O11-Dy4-O8	100.6(3)
O11-Dy1-O2	135.3(3)	O17-Dy2-N2	124.2(3)	O10-Dy4-O13	85.5(2)
O1-Dy1-O18	95.8(3)	O4-Dy2-O15	86.6(3)	O8-Dy4-O13	77.6(2)
O2-Dy1-O18	80.7(3)	N2-Dy2-O15	152.5(3)	O11-Dy4-O15	73.7(3)
O1-Dy1-O15	138.9(3)	O13-Dy2-N5	64.9(3)	O13-Dy4-O15	74.9(2)
O2-Dy1-O15	74.1(2)	O17-Dy2-N5	129.7(3)	O10-Dy4-N8	77.6(3)
O18-Dy1-N1	90.7(3)	O7-Dy3-O19	98.6(3)	O11-Dy4-N8	87.9(3)
O15-Dy1-N1	130.2(3)	O5-Dy3-O19	83.7(3)	O13-Dy4-N8	108.2(3)
O1-Dy1-O17	137.6(3)	O19-Dy3-N3	85.2(3)	O15-Dy4-N8	65.7(3)
O11-Dy1-O17	71.7(3)	O19-Dy3-N6	170.6(3)	O10-Dy4-N4	72.6(3)
O4-Dy2-O13	126.3(2)	N6-Dy3-O13	64.1(2)	O11-Dy4-N4	69.1(3)
O5-Dy2-O13	74.6(2)	O7-Dy3-O17	141.1(3)	O15-Dy4-N4	132.4(3)
O2-Dy2-O13	132.7(2)	O10-Dy4-O8	85.5(3)	N4-Dy4-O17	125.9(3)

Symmetry code: 2-x, -0.5+y, 2.5-z

**Table S3.** Selected bond lengths (Å) and angles (°) for **2**.

Selected bond lengths for <b>2</b>					
Dy1-O16	2.267(6)	Dy2-O5	2.344(7)	Fe2-O12	1.975(6)
Dy1-O3	2.280(6)	Dy2-O18	2.430(6)	Fe2-O5	2.023(7)
Dy1-O12	2.290(6)	Dy2-O6	2.463(6)	Fe2-N2	2.090(8)
Dy1-O18	2.374(6)	Dy2-N4	2.598(9)	Fe2-N8	2.244(9)

Dy1-O9	2.393(6)	Fe1-O1	1.938(7)	Fe3-O11	1.929(7)
Dy1-O2	2.424(6)	Fe1-O18	1.941(7)	Fe3-O9	2.024(6)
Dy1-N5	2.512(8)	Fe1-O3	2.004(7)	Fe3-N6	2.181(8)
Dy1-O10	2.523(6)	Fe1-O7	2.005(7)	Fe3-N7	2.198(8)
Dy2-O16	2.292(6)	Fe1-N1	2.103(8)	Fe4-O13	1.883(8)
Dy2-O7	2.293(7)	Fe1-N3	2.223(9)	Fe4-O17	1.939(7)
Dy2-O14	2.332(7)	Fe2-O18	1.927(7)	Fe4-O14	1.959(7)
Dy2-O17	2.343(7)	Fe2-O4	1.963(7)	Fe4-N9	2.084(9)

Selected bond angles for <b>2</b>					
O16-Dy1-O3	104.5(2)	O16-Dy2-N4	80.0(2)	O11-Fe3-N7	78.1(3)
O3-Dy1-O-12	133.9(2)	O7- Dy2-N4	63.1(3)	O11-Fe3-Cl1	101.8(2)
O16-Dy1-O18	71.0(2)	O18-Dy2-N4	114.8(2)	N7-Fe3-Cl1	87.8(2)
O16-Dy1-O9	92.4(2)	O1-Fe1-O18	96.6(3)	O11-Fe3-Cl2	98.8(2)
O3-Dy1-O2	76.2(2)	O18-Fe1-O3	87.0(3)	N7-Fe3-Cl2	176.9(2)
O16-Dy1-N5	80.4(2)	O18-Fe1-O7	84.1(3)	Cl1-Fe3-Cl2	92.73(11)
O3-Dy1-N5	81.1(2)	O18-Fe1-N1	109.3(3)	O13-Fe4-O17	96.1(3)
O16-Dy1-O10	137.6(2)	N1-Fe1-N3	92.5(3)	O13-Fe4-O14	136.7(4)
O16-Dy2-O7	100.8(2)	O18-Fe2-O4	95.6(3)	O17-Fe4-O14	81.3(3)
O16-Dy2-O14	142.6(2)	O4-Fe2-O12	94.6(3)	O13-Fe4-N9	87.5(3)
O7-Dy2-O17	144.3(2)	O12-Fe2-O5	99.1(3)	O14-Fe4-N9	79.5(3)
O16-Dy2-O5	85.5(2)	O5-Fe2-N2	80.2(3)	O13-Fe4-Cl3	108.6(3)
O16-Dy2-O18	69.6(2)	N2-Fe2-N8	89.1(3)	O17-Fe4-Cl3	101.8(2)
O5-Dy2-O18	68.9(2)	O11-Fe3-O9	88.4(3)	O14-Fe4-Cl3	114.3(3)

Symmetry code: 0.5-x, 1.5-y, -z

**Table S4.** Bond valence sum (BVS) calculations for determining of the protonation levels of the O atoms in **1** and **2**.

Atoms in <b>1</b>	BVS values of <b>1</b>	Atoms in <b>2</b>	BVS values of in <b>2</b>
O1	1.95	O1	1.78
O2	1.88	<b>O2</b>	<b>1.29</b>
<b>O3</b>	<b>0.88</b>	O3	1.93
O4	1.77	O4	1.75

O5	1.96	O5	1.78
O6	0.88	O6	1.17
O7	1.85	O7	2.04
O8	1.98	O8	1.83
O9	0.87	O9	1.91
O10	1.70	O10	1.13
O11	1.89	O11	1.61
O12	0.81	O12	2.03
O13	1.85	O13	1.90
O14	0.82	O14	1.96
O15	1.84	O15	0.87
O16	0.90	O16	1.90
O17	2.27	O17	1.90
O18	1.91	O18	1.99
O19	1.91		

The values of BVS calculations for O atoms in the ~1.8–2.0, ~1.0–1.2, and ~0.2–0.4 ranges are indicative of non-, single- and double-protonation, respectively. Single protonated alkoxido-type O atoms on the organic ligands were labelled using red.

**Table S5.** Bond valence sum (BVS) calculations for determining of the oxidation of the Fe atoms in **2**.

Fe atom in complex <b>2</b>	Fe(II)	Fe(III)
Fe(1)	2.81	<u>3.05</u>
Fe(2)	2.21	<u>3.05</u>
Fe(3)	2.63	<u>2.87</u>
Fe(4)	2.83	<u>3.06</u>

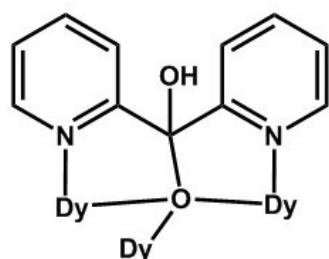
**Table S6.** The possible geometries of oct-coordination metal centers and Deviation parameters from each ideal polyhedron for Dy of complex **1**.

Point group	Geometry	Polyhedron	Dy1	Dy2	Dy3	Dy4
$D_{8h}$	OP-8	Octagon	33.085	27.492	33.598	38.719
$C_{7v}$	HPY-8	Heptagonal pyramid	23.594	22.589	23.636	22.734
$D_{6h}$	HBPY-8	Hexagonal bipyramid	14.977	16.615	13.955	15.988
$O_h$	CU-8	Cube	12.620	11.118	10.445	11.783
$D_{4d}$	SAPR-8	Square antiprism	4.678	1.441	4.189	1.926

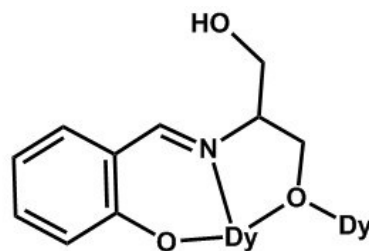
$D_{2d}$	TDD-8	Triangular dodecahedron	2.977	2.612	3.345	1.959
$D_{2d}$	JGBF-8	Johnson - Gyrobifastigium (J26)	11.110	14.046	10.845	12.464
$D_{3h}$	JETBPY-8	Johnson - Elongated triangular bipyramid (J14)	25.019	24.337	26.673	25.933
$C_{2v}$	JBTP-8	Johnson - Biaugmented trigonal prism (J50)	3.049	2.256	3.318	1.951
$C_{2v}$	BTPR-8	Biaugmented trigonal prism	2.950	2.100	3.076	2.022
$D_{2d}$	JSD-8	Snub disphenoid (J84)	3.729	4.368	3.704	3.290
$T_d$	TT-8	Triakis tetrahedron	12.892	11.399	10.845	12.042
$D_{3h}$	ETBPY-8	Elongated trigonal bipyramid	21.059	21.171	22.232	22.504

**Table S7.** The possible geometries of oct-coordination metal centers and Deviation parameters from each ideal polyhedron for Dy of complex **2**.

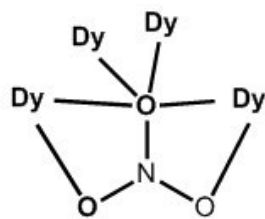
Point group	Geometry	Polyhedron	Dy1	Dy2
$D_{8h}$	OP-8	Octagon	30.679	33.839
$C_{7v}$	HPY-8	Heptagonal pyramid	20.359	23.253
$D_{6h}$	HBPY-8	Hexagonal bipyramid	14.400	12.255
$O_h$	CU-8	Cube	9.503	7.841
$D_{4d}$	SAPR-8	Square antiprism	1.988	3.171
$D_{2d}$	TDD-8	Triangular dodecahedron	2.283	1.533
$D_{2d}$	JGBF-8	Johnson - Gyrobifastigium (J26)	14.478	13.781
$D_{3h}$	JETBPY-8	Johnson - Elongated triangular bipyramid (J14)	25.365	25.988
$C_{2v}$	JBTP-8	Johnson - Biaugmented trigonal prism (J50)	2.539	3.692
$C_{2v}$	BTPR-8	Biaugmented trigonal prism	2.487	3.366
$D_{2d}$	JSD-8	Snub disphenoid (J84)	4.754	3.860
$T_d$	TT-8	Triakis tetrahedron	10.351	8.230
$D_{3h}$	ETBPY-8	Elongated trigonal bipyramid	22.772	20.965



Coordination mode  $\eta^1, \eta^1, \eta^3: \mu_3$

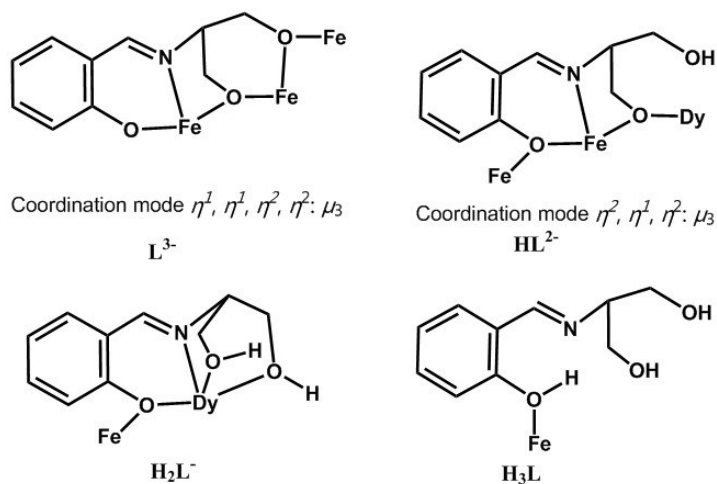


Coordination mode  $\eta^1, \eta^1, \eta^2: \mu_2$



Coordination mode  $\eta^2, \eta^1, \eta^1, \mu_4$

**Scheme S1.** The coordination modes of  $(\text{py})_2\text{C}(\text{OH})\text{O}^-$ ,  $\text{HL}^{2-}$  and  $\text{NO}_3^-$  with metals for **1**.



**Scheme S2.** The coordination modes of  $\text{L}^{3-}$ ,  $\text{HL}^{2-}$ ,  $\text{H}_2\text{L}^-$  and  $\text{H}_3\text{L}$  in the complexes with the formula  $[\text{Fe}^{\text{III}}_4\text{Ln}^{\text{III}}_2(\text{H}_2\text{L})_2(\text{HL})_2\text{L}_2(\text{CH}_3\text{OH})_2((\text{CH}_3)_3\text{CCOO})_2(\text{NO}_3)_2][\text{Ln}^{\text{III}}(\text{NO}_3)_4(\text{H}_3\text{L})(\text{CH}_3\text{OH})]_3 \cdot \text{NO}_3 \cdot 3\text{H}_2\text{O}$  reported by J. Reedijk *et al.*

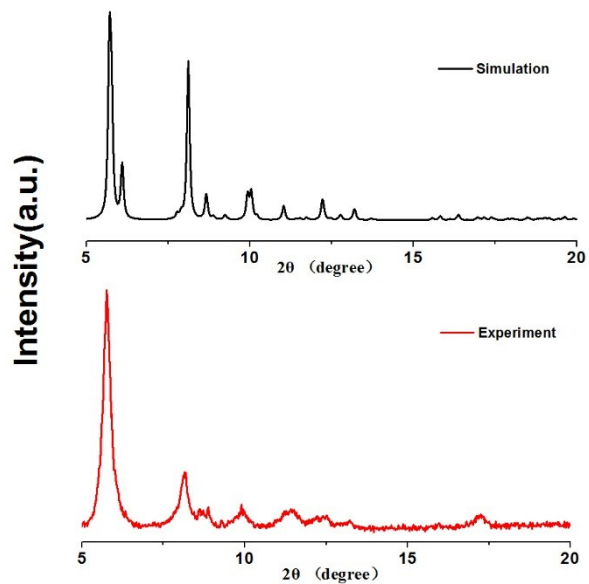


**Figure S1.** PXRD patterns and simulated patterns generated from single crystal diffraction data for compound **1**.

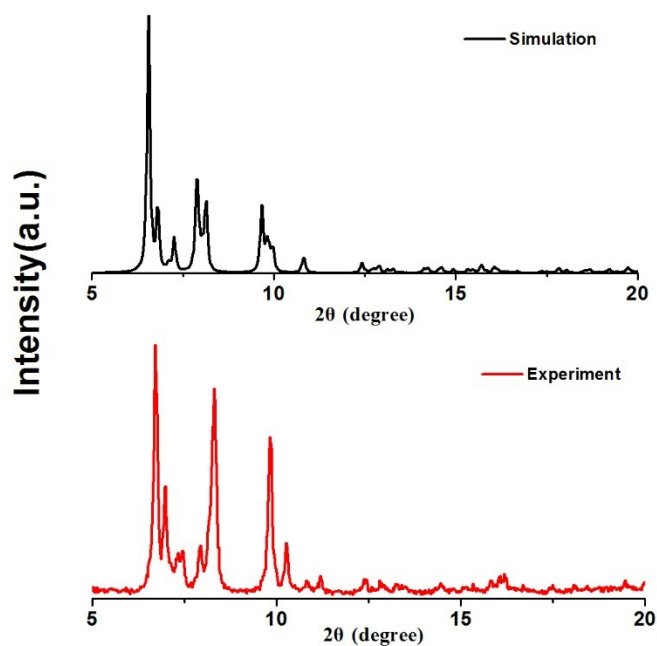


**Figure S2.** PXRD patterns and simulated patterns generated from single crystal diffraction data for compound **2**.

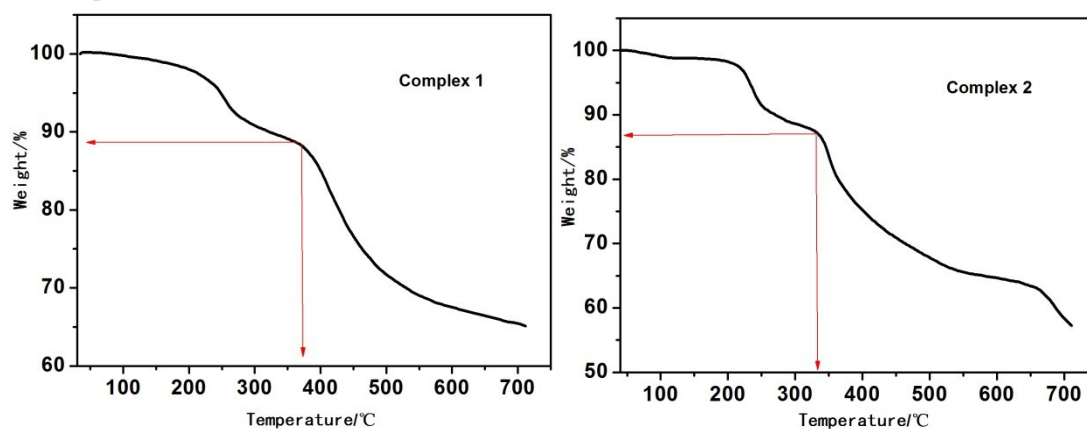


**Figure S3.** Plots of TGA for complexes **1** (left) and **2** (right). The red arrows were directed the weight losses or temperatures to see easily.

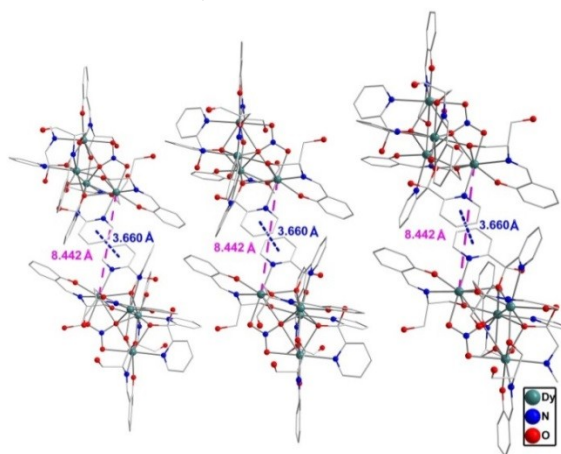


**Figure S4.** The plot shows the  $\pi$ - $\pi$  packing interactions and the shortest distances of Dy<sup>III</sup>...Dy<sup>III</sup> between the nearest neighboring molecules of **1**. For clarity, the H atoms and solvent molecules were omitted.



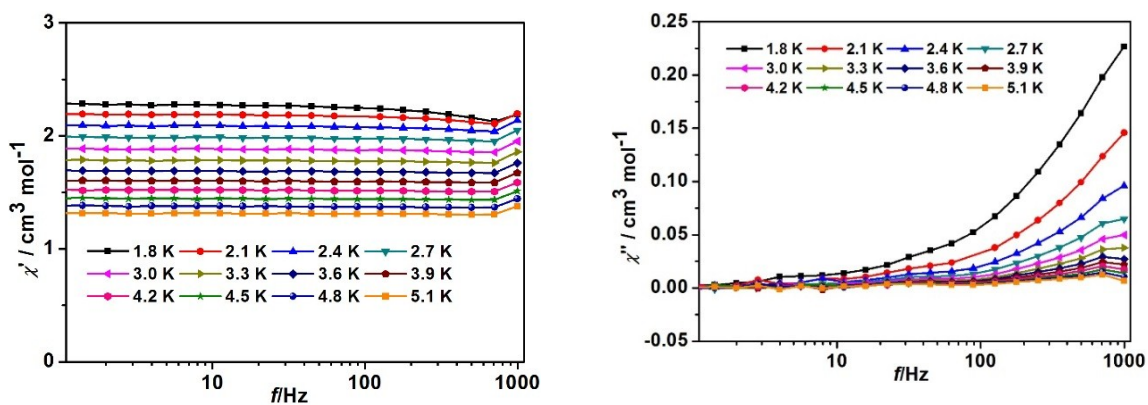


**Figure S8.** Plots of in-phase ( $\chi'$ ) versus  $f$  (left) and out-of-phase ( $\chi''$ ) versus  $f$  (right) for **1** with a zero applied dc field.

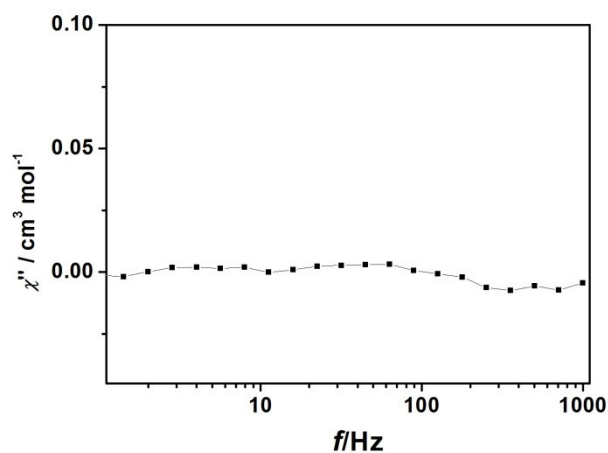


**Figure S9.** Frequency dependence of the out-of-phase ( $\chi''$ ) ac magnetic susceptibilities for **2** collected under a 0 Oe dc field with the temperature 1.8.

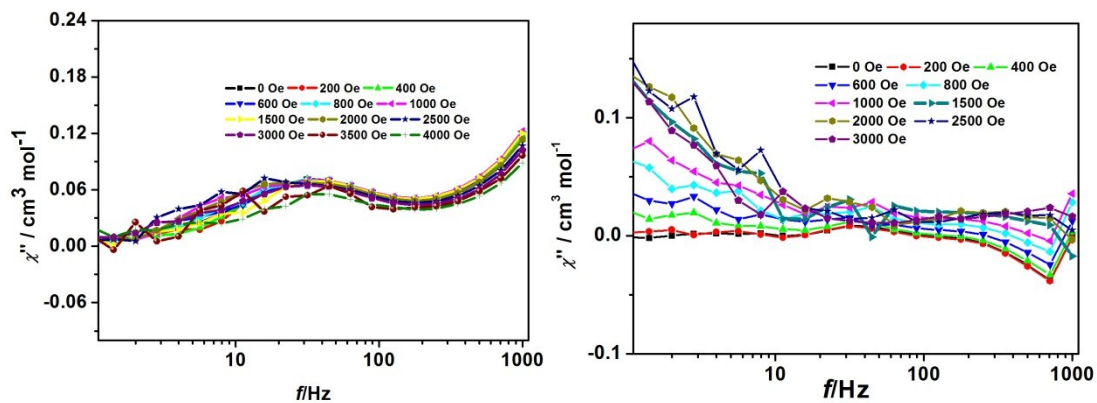


**Figure S10.** Plots of out-of-phase ( $\chi''$ ) versus  $f$  for **1** (left) at 2.0 K and for **2** (right) at 1.8 K with the applied dc field shown in plots.

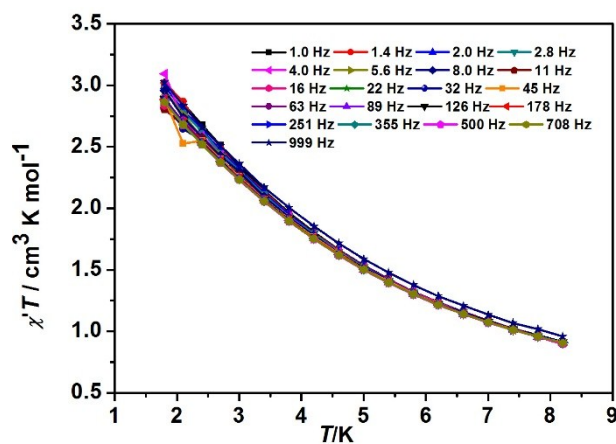


**Figure S11.** Plots of in-phase ( $\chi'$ ) versus  $T$  for **2** under a dc field of 1500 Oe.

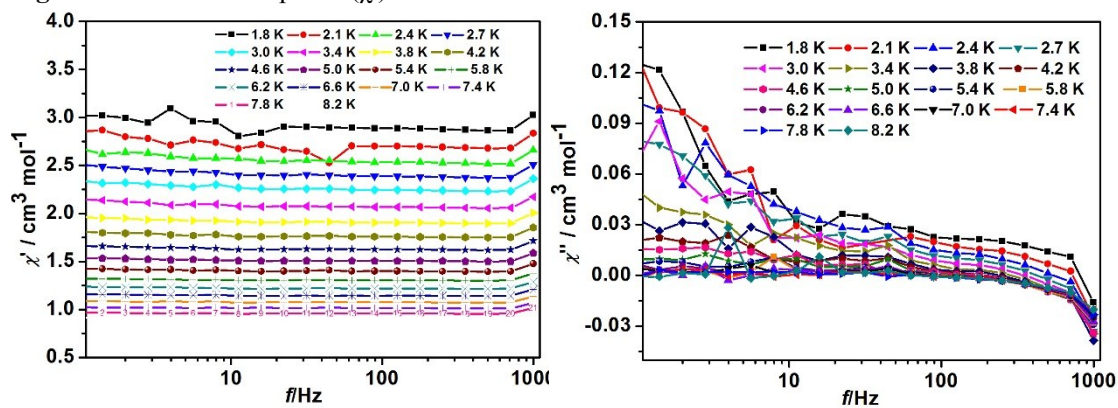


**Figure S12.** Plots of in-phase ( $\chi'$ ) versus  $f$  (left) and out-of-phase ( $\chi''$ ) versus  $f$  (right) for **2** under a dc field of 1500 Oe.